scientific reports

Check for updates

OPEN

Synthesis and characterization of innovative GA@Ag-CuO nanocomposite with potent antimicrobial and anticancer properties

Amr H. Hashem[1]✉, Mostafa A. Abdel-Maksoud[2], Sabiha Fatima[3], Saeedah M. Almutairi[2], Mohamed A. Ghorab[4,5], Ahmed I. El-Batal[8] & Gharieb S. El-Sayyad[6,7,8]✉

Cancer and microbial infections place a significant burden on the world's health systems and can increase the rate of disease and mortality. In the current study, a novel nanocomposite based on Gum Arabic, silver and copper oxide nanoparticles (GA@Ag-CuO nanocomposite) was synthesized to overcome the problem of microbial infection and in cancer treatment. Characterization using UV-Vis. spectrophotometer reveals that, the observed peak in the spectrum was formed by the observed O.D. at 0.755, and confirmed that the produced GA@Ag-CuO nanocomposite was small and discernible at 360 nm. The particles' diameters varied from 9.5 nm to 49.5 nm, with a mean diameter of 25.53 ± 1.4 nm. The created Gum Arabic filtrate was rich in active functional groups, and the provided polydisperse NPs were intended to reduce, stabilize, and the produced filtrate act as capping agents. Based on the XRD data, the synthesized GA@Ag-CuO nanocomposite was crystallized and had a face-centered (fcc) crystal structure. Biosafety of GA@Ag-CuO nanocomposite was assessed toward Wi 38 normal cell line, where it showed safety toward the tested cell line where IC50 was 154.2 µg/mL. Antimicrobial results confirmed that, GA@Ag-CuO nanocomposite has antibacterial activity with MICs 15.6, 125, 31.25 and 125 µg/mL against *S. epidermis*, *S. aureus*, *L. plantrum*, and *S. typhimurium*, respectively. Likewise, it showed antifungal activity toward *C. albicans* and *C. neoformans* with MICs 62.5 and 15.62 µg/ml, respectively. Moreover, GA@Ag-CuO nanocomposite displayed promising anticancer activity with IC_{50} 26.11 and 59.5 µg/ml toward MCF-7 and Hep-G2, respectively. In conclusion, the novel GA@Ag-CuO nanocomposite demonstrated promising antibacterial, antifungal, and anticancer activities.

Keywords Gum arabic, Bimetallic Ag-CuO NPs, Antimicrobial potential, Anticancer activity

Microbial infections are caused by microorganisms such as bacteria, viruses, fungi, and parasites, and can lead to a wide range of diseases and health complications[1,2]. These infections impose a substantial strain on global health systems and can lead to elevated rates of illness and death[3,4]. Effective treatment of microbial infections relies heavily on the use of antimicrobial drugs, which target and eliminate the causative microorganism[5,6]. Nevertheless, the rise and dissemination of antimicrobial resistance (AMR) have evolved into a significant

[1]Botany and Microbiology Department, Faculty of Science, Al-Azhar University, Nasr City 11884, Cairo, Egypt. [2]Department of Botany and Microbiology, College of Science, King Saud University, P.O. Box 2455, Riyadh 11451, Saudi Arabia. [3]Department of Clinical Laboratory Science, College of Applied Medical Sciences, King Saud University, P.O. Box 10219, Riyadh 11433, Saudi Arabia. [4]Wildlife Toxicology Lab, Dept. of Animal Science, Institute for Integrative Toxicology (IIT), Michigan State University, East Lansing, MI 48824, USA. [5]School of Veterinary Medicine, Department of Molecular Biosciences, University of California, Davis, CA 95616-8741, USA. [6]Department of Medical Laboratory Technology, Faculty of Applied Health Sciences Technology, Badr University in Cairo (BUC), Badr city, Cairo, Egypt. [7]Department of Microbiology and Immunology, Faculty of Pharmacy, Galala University, New Galal City, Suez, Egypt. [8]Drug Microbiology Lab, Drug Radiation Research Department, National Center for Radiation Research and Technology (NCRRT), Egyptian Atomic Energy Authority (EAEA), Cairo, Egypt. ✉email: amr.hosny86@azhar.edu.eg; Gharieb.Elsayyad@gu.edu.eg

worldwide health emergency[7]. Antimicrobial resistance (AMR) is the capacity of microorganisms to persist and reproduce when exposed to antimicrobial medications that were initially successful against them[8]. This condition makes previously successful treatments ineffective, resulting in longer periods of sickness, higher healthcare expenses, and increased mortality rates[8]. Current antimicrobial therapies face several drawbacks, including the emergence of antibiotic resistance[9]. Bacteria are rapidly evolving, developing resistance to existing antibiotics, making infections increasingly difficult to treat. This necessitates the development of new antimicrobial agents with novel mechanisms of action. Additionally, many antibiotics have undesirable side effects, impacting the gut microbiome and potentially leading to allergic reactions. The narrow spectrum of activity of many antibiotics also limits their effectiveness against a wide range of pathogens[10,11].

Cancer cells often acquire resistance to medications intended to eradicate them, posing a major issue in the area of oncology known as anticancer resistance[12]. Resistance can arise through different processes, including as genetic mutations, changes in drug targets, activation of alternative signaling pathways, and improved DNA repair mechanisms[13]. It results in the failure of treatment, the advancement of the disease, and a restricted range of treatment choices for individuals with cancer[14]. Cancer therapies, while showing progress, still face significant limitations. Current treatments, such as chemotherapy and radiation, often have severe side effects, compromising the patient's overall health and quality of life[11]. These therapies can also target healthy cells, leading to complications and further weakening the immune system. Moreover, many cancers develop resistance to existing treatments, necessitating the development of new and more targeted therapies[15]. The high cost of many cancer treatments also poses a significant barrier to access for many patients[11]. Gaining insight into the mechanisms that cause resistance to anticancer treatments is essential for enhancing the effectiveness of cancer therapies[16]. Scientists are currently studying the molecular and cellular mechanisms that cause resistance, aiming to discover techniques to overcome it[17]. This encompasses the advancement of combination medicines, targeted therapies, and immunotherapies that have the ability to bypass or reverse resistance mechanisms[18].

In the battle against microbial infections and tumor therapy, the use of nano-biotechnology in pathogen resistance and cancer pandemic reduction has shown notable and durable results. This is due to the fact that nanotechnology enables improved attraction to fungus, and bacterial cells, through the generation of reactive oxygen species (ROS) which stimulates their inhibition[19–21]. Entire biological components have been included in the scope of biological methods to nanoparticles and nano-crystal production[22,23]. The use of macromolecules that are plants, bacteria, cyanobacteria, and fungi or other agricultural and industrial wastes as agreen materials in the biological synthesis of metal NPs has garnered significant interest recently due to its environmental friendliness and safety[24–33]. Natural polymeric cap agents, such as chitosan and gum Arabic, are used to regulate the inorganic polymer NPs' particle size and improve their stability[34,35]. Gum Arabic is different from other macromolecules in biology in that it has a variety of attractive features that make it a preferred option for the production of bimetallic nano-materials[9]. These crucial attributes are lower toxicity, biological compatibility, affordability, and availability[36].

Nanocomposites, materials composed of two or more components at the nanoscale, have emerged as promising candidates for biomedical applications[37]. The unique properties of these materials, such as their high surface area, enhanced mechanical strength, and tunable surface chemistry, offer significant advantages over conventional materials[38]. For instance, nanocomposites can be designed to deliver drugs specifically to target cells, improving therapeutic efficacy and minimizing side effects. They can also be used as biocompatible coatings for implants, promoting tissue regeneration and reducing the risk of infection[39,40].

Nanocomposites are revolutionizing antimicrobial and cytocompatibility applications due to their unique properties[41]. Their high surface area allows for increased contact with microbes, enhancing their antimicrobial efficacy. Additionally, the incorporation of antimicrobial agents within the nanocomposite structure can provide sustained release, prolonging their activity[42,43]. These materials can also be designed to be biocompatible, minimizing cytotoxicity and promoting cell adhesion and proliferation This makes them ideal for applications like wound dressings, implantable devices, and drug delivery systems, where both antimicrobial and cytocompatibility are crucial for successful outcomes[44].

Bimetallic nanomaterials are receiving a lot of attention because of the distinctive chemical, physical, and physiological characteristics that result from the combination of several metal elements[35,45–54]. Bimetallic GA@Ag-CuO nanocomposite offer a unique combination of properties that make them promising for various biological applications. Their enhanced antimicrobial activity, stemming from the synergistic action of silver and copper ions, combats a broader spectrum of microorganisms, including antibiotic-resistant strains[55,56]. These nanoparticles can also be functionalized for targeted drug delivery, enhancing therapeutic efficacy while minimizing side effects[57], and in the treatment of some infectious diseases like foot and mouth disease (FMD)[54]. Their photothermal properties hold potential for cancer treatment, while their anti-inflammatory and antibacterial effects promote wound healing[58].

Herein, the main aim of this study was to synthesize a novel nanocomposite based on Gum Arabic, silver, and copper oxide nanoparticles (GA@Ag-CuO nanocomposite), characterize it, and assess its biosafety, antimicrobial, and anticancer activities.

Materials and methods

Chemicals and reagents

To produce the bimetallic nanoparticles for the investigation, analytical-grade chemicals were acquired from Sigma Aldrich in the UK. These included Gum Arabic; purity 99% (Meron Company, India), silver nitrate; purity 99.9% (Ag NO_3), and copper acetate; purity 97% (Cu $(CH_3COO)_2$. Furthermore, the microbiological examination medium used in the antimicrobial experiment, and other materials in anticancer test were supplied by Oxide (UK).

Green synthesis of GA@Ag-CuO nanocomposite

The exact concentration of the utilized salts (silver nitrate, and copper acetate) was used to synthesize GA@Ag-CuO nanocomposite. Specifically, 10 mL of Ag NO_3 (2.0 mM) and 10 mL of $Cu(CH_3COO)_2$ (2.0 mM) were combined together in a 250 mL Erlenmeyer conical flask at room temperature for half an hour (Scheme 1). After that, 80 mL of the 20% Gum Arabic had been added drop-wise which used as a reducing and stabilizing agent. After combining the two solutions, we measured the combination's pH and found to be 7.1.

The reaction conditions were selected to consist of temperature-controlled incubating at 30 °C and a 24-hour reaction period under rotation (500 rpm) in a shaking incubator in order to obtain the most efficient synthesis of Ag-CuO NPs (Scheme 1)[59].

The optical density (OD) of the produced bimetallic NPs was measured using UV-Vis. spectrophotometer to determine the possibility of the preparation. After that, the produced GA@Ag-CuO nanocomposite was washed with distilled water, centrifuge (5000 rpm) to collect the solid materials, then dried in oven at 80 °C for about 12 h for preparing the powder GA@Ag-CuO nanocomposite for the next characterization methods (Scheme 1).

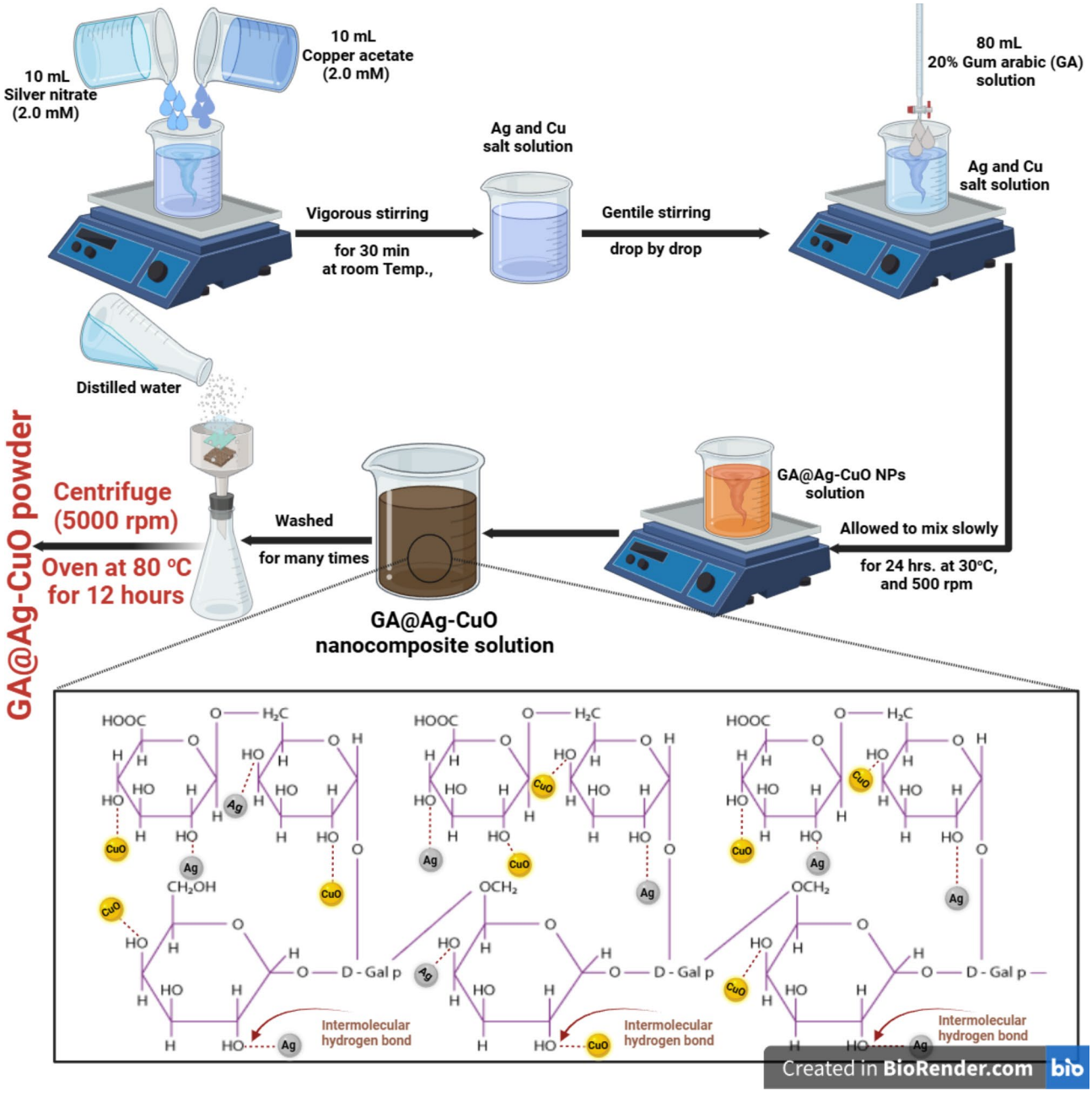

Scheme 1. Illustrated scheme regarding step by step preparation of GA@Ag-CuO nanocomposite, created by BioRender.com.

Characterization of the synthesized GA@Ag-CuO nanocomposite

A JASCO V-560 UV-Vis. spectrophotometer was utilized to investigate the absorption and spectral characteristics of GA@Ag-CuO nanocomposite that were synthesized at particular wavelengths ranged from 190 to 900 nm. Another step experiment devoid of any metal ions was offered for Auto-zero reasons. First, each specimen's optical characteristics were examined to ascertain the overall number of wavelengths required to estimate absorbance.

Conducing the DLS-PSS-NICOMP 380-ZLS particle-sized equipment at the St. Barbara, California, USA facility, dynamic light scattering measurements were used to determine the mean size distribution of the synthesized GA@Ag-CuO nanocomposite. Samples of tested GA@Ag-CuO nanocomposite (100 µL) were briefly contained in a small cuvette. Following two minutes of equilibrium at 25.0 ± 2 °C ambient temperature, the procedures were performed three times.

The synthesized GA@Ag-CuO nanocomposite's size, form, and overall appearance were evaluated with a high-resolution transmission electron microscope (HR-TEM, JEM2100, Jeol, Japan). Additionally, the XRD-6000 lists, Shimadzu equipment, and SSI, Japan made it possible to examine the formed crystals, and crystallite sizes of the synthesized GA@Ag-CuO nanocomposite. The diffracted angle of 2θ was utilized to determine the X-ray power. A scanning electron microscope (SEM, ZEISS, EVO-MA10, Germany) was used to examine the formed Ag-CuO NPs surrounding GA in order to evaluate their surface form and arrangement. Finally, the surface charges of the produced GA@Ag-CuO nanocomposite were informally evaluated at the pH of preparation using a Zeta potential analyzer (they were performed in triplicate ($n = 3$)) from Malvern Device, UK[60].

Antimicrobial activity

The antimicrobial activity of GA@Ag-CuO nanocomposite, silver nitrate, copper acetate against *Staphylococcus epidermis ATCC* 14,990, *Staphylococcus aureus* ATCC 25,922, *Lactobacillus plantrum* ATCC 8014, *Salmonella typhimurium* ATCC 14028 *Candida albicans* ATCC 90028, and *C. neoformans* ATCC 14116 was evaluated using the agar well diffusion technique[61]. GA@Ag-CuO nanocomposite, silver nitrate, and copper acetate were added to agar wells at a concentration of 1000 µg/mL. Additionally, a standard antibiotic (Ampicillin/sulbactam 20) as positive control was included. The mixture was then incubated at 37 °C for 24 h, allowing for observation and analysis. Alternatively, fungal strains were cultured on PDA plates and placed in an incubator at 30 °C for 3–5 days. The fungal suspension was prepared in a sterilized phosphate buffer solution (PBS) with a pH of 7.0. After counting in a cell counter chamber, the inoculums were adjusted to a concentration of 10^7 spores per milliliter. The distribution of one milliliter was done evenly across agar PDA Plates. Next, 100 µl of the tested GA@Ag-CuO nanocomposite, silver nitrate, copper acetate at a concentration of 1000 µg/mL, and the reference antifungal (Nystatin 100) as positive control were put. Following incubation at 30 °C for 72 h, the diameter of the inhibition zone was measured. In order to determine the minimum inhibitory concentration, a solution of GA@Ag-CuO nanocomposite was prepared in various concentrations, ranging from 1000 to 3.9 µg/mL. These concentrations were then tested individually against specific bacterial and fungal strains[62–64].

Cytotoxicity

The cytotoxicity of GA@Ag-CuO nanocomposite and Taxol as positive control was determined using the MTT protocol[65] with minor modifications. The normal Wi38 and cancerous MCF7 cell lines were collected from American type culture collection (ATCC). The optical density was measured at 560 nm. The cell quantity and the percentage of viable cell were totaled by the following formula:

$$Viability\,\% = \frac{Test\,OD}{Control\,OD} \times 100$$

$$Inhibition\,\% = 100 - Viability$$

Results and discussion

Synthesis and characterization of GA@Ag-CuO nanocomposite

Gum Arabic's ability to create Ag-CuO NPs as a capping and reducing agent was assessed. When the bimetallic Ag-CuO NPs were produced, the resulting solution's initially pale-yellow tint turned to a deep brown hue. As a dependable spectroscopic sign of their presence, the deep brown color that resulted was related to the stimulation of the surface Plasmon resonance which happens in GA@Ag-CuO nanocomposite[66,67].

The observed peak in the spectrum (Fig. 1) was formed by the observed OD at 0.755, and the UV-Vis. investigations revealed that the produced GA@Ag-CuO nanocomposite (diluted 5 times) were small and discernible at 360 nm. Conversely, Fig. 1 showed the UV-Vis. spectra of the initial precursors, silver nitrate and copper acetate, which had distinct wavelengths; silver nitrate at 283 nm[68] and copper acetate at 203 nm[69].

The ability to produce Ag-CuO NPs by biosynthesis was associated with the depth of the deep brown color[70–72]. Surface Plasmon resonance (SPR) is frequently impacted by the size, morphology, dielectric properties, and structure of every generated nanoparticles[73,74].

The longest-term stability of the generated NPs due to GA's capping capacity, which enhanced their properties for prospective long-term applications in the pharmaceutical, cosmetic, and plant protection industries, is the scientifically sound aspect of this study[75–78].

According to the literature[35], the FTIR results revealed peak absorption values at 3291 cm^{-1} (attributed to –OH), 2985 cm^{-1} (symmetric and asymmetric –CH vibration), 1642 cm^{-1} (attributed to –COOH), 1462 cm^{-1} (uronic acid symmetrically stretched by carboxylic groups), 1066 cm^{-1} (perhaps due to arabinogalactan), and 890.0 cm^{-1} (attributed to galactose 1–4 linkage and mannose 1–6 linkage). The same peaks in the metal NPs spectra indicate that GA was successful in capping. Moreover, the galactose/mannose peak became less

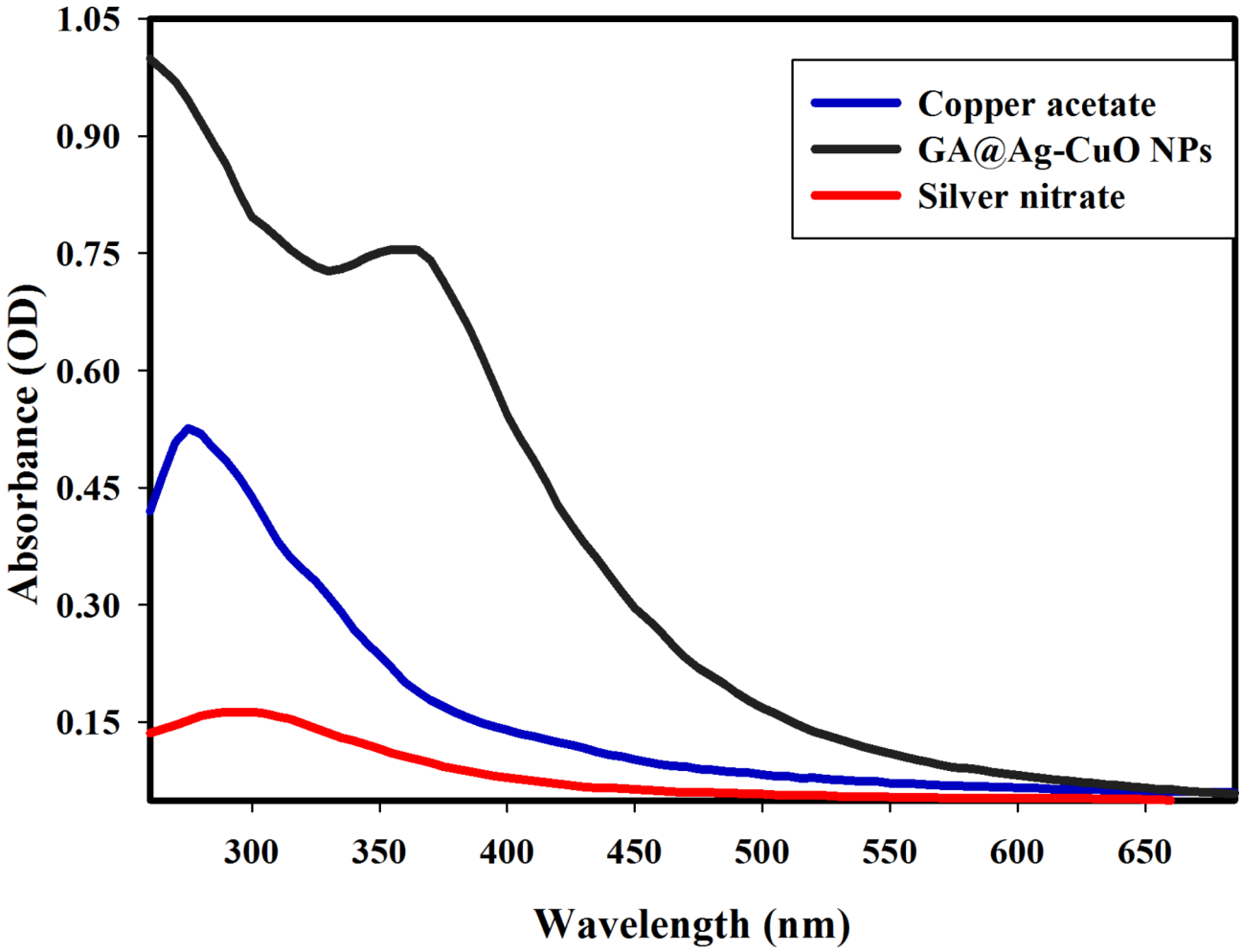

Fig. 1. UV-Vis. spectrum of copper acetate, silver nitrate, and the synthesized GA@Ag-CuO nanocomposite (diluted 5 times).

prominent and the arabinogalactan peak lost its doublet. Additionally, a clear peak at 715.25 cm^{-1} was seen, which may be the outcome of metal NPs interacting and combining with hydroxyl groups to create metal–O[79].

According to El-Batal, et al.,[35] results, all of the peaks were in identical wavenumbers, suggesting that the synthesized NPs were similarly incorporated and/or conjugated through the primary functional groups of the stabilizer GA. The lack of noise and additional unidentified peaks indicated the high purity of the synthesized sample[78].

The consequent GA@Ag-CuO nanocomposite' hydrodynamic width, particle size dispersion, and polydispersity index (PDI) were measured using DLS analysis. The average size of the produced nanoparticles was ascertained by contrasting the acquired data to the HR-TEM investigation[80].

The generated GA@Ag-CuO nanocomposite was shown to be semi-spherical and connected to supporting gum Arabic in Fig. 2a's HR-TEM image. With an average width of 25.53 ± 1.4 nm, the particles' sizes ranged from 9.5 nm to 49.5 nm (Fig. 2a). The generated Gum Arabic filtrate was full of active groups that were functional, and the polydisperse NPs were added with the intention of, among other things, stabilizing, reducing, and capping the filtrate[81].

Ag and Cu may decrease concurrently as a result of the radical-multi-position of gum Arabic produced, as described and compared in the study given. The HR-TEM image output (Fig. 2a) demonstrated uniform line spacing, which resulted in a single grade system, and copper equally distributed throughout the zinc matrix, resulting in a unique alloy[35].

Using the SEM approach, the surface characteristics and surface form of the generated synthetic nanoparticles were examined. The produced Gum Arabic included the matching bright spherical particles, and the ZnO-Ag NP surfaces seem clear when seen in combination with the Gum Arabic SEM data (Fig. 2b). It was found that the produced Gum Arabic, which looks as lighted NPs fused and capped with it, effectively separated the GA@Ag-CuO nanocomposite as spheroidal particles united with one another (Fig. 2b). In contrast to previous studies on the topic of morphological shape, the Ag-CuO NPs produced in this work had a precise spherical formation, a confined size, and an even distribution. Mohsin et al.[82] used the citrate reduction process to create bimetallic silver-gold nanoparticles at different pH and temperature levels. Since the permitted morphological form and

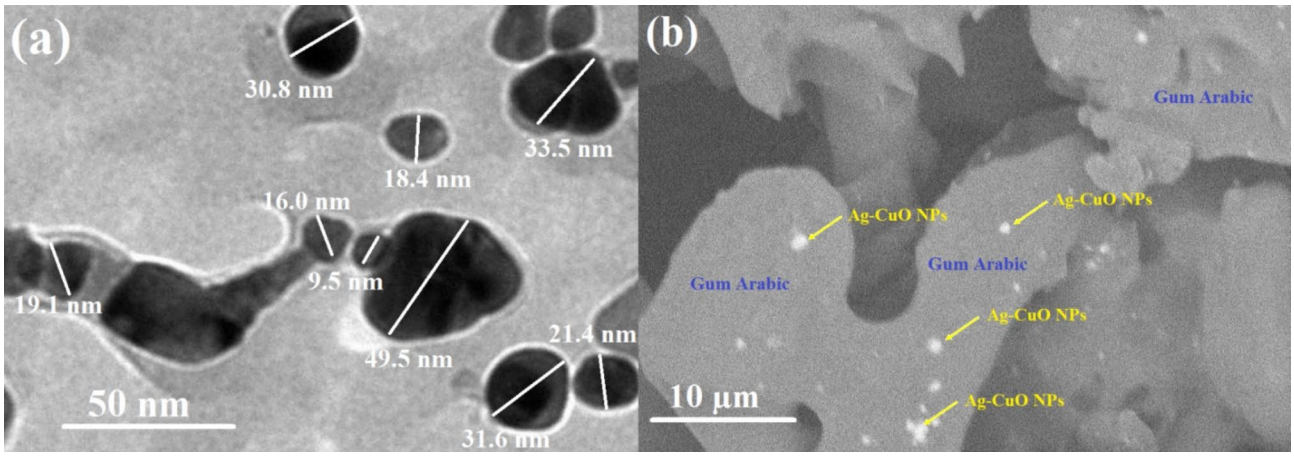

Fig. 2. HR-TEM images (**a**), and SEM images of the synthesized GA@Ag-CuO nanocomposite (**b**).

border size indicated that they keep the size range around 50 and 65 nm while seeming like spheroidal particles, pH and temperature play a crucial role in the synthetic process.

Our mixture of Ag-CuO NPs was found to be polydisperse NPs, differed in size, and mostly possessed spherical particles as their primary shape after comparing them to articles in the literature on medium particle size and form. Although the produced NPs were essentially spherical or orbicular in shape, the process of creating them from extract may have produced a variety of morphologies, which explains why the asymmetrical form was observed. A permanent form is polydisperse NPs since in our study we only utilized the most practical reducing and covering agent (Gum Arabic)[83]. The role of Gum Arabic as a stabilizing agent had been confirmed in the literature, since El-Batal et al.,[35], utilized the Gum Arabic as a stabilizing agents when synthesized bimetallic Ag-Au NPs and according to their FTIR data they confirm the incorporation of the synthesized bimetallic Ag-Au NPs with the stabilizer Gum Arabic as in our related study.

As shown in Fig. 3a, the particle size distribution (PSD) for bimetallic Ag-CuO NPs, which were produced using gum Arabic, was determined to be 55.42 ± 2.3 nm using the DLS technique (they were performed in triplicate ($n = 3$).

Samples are considered monodisperse by the International Standards Organizations (ISOs) if the polydispersity index (PDI) findings are less than 0.05. On the other hand, particles with a variability distribution are supposed to be produced when PDI results exceed 0.7[84]. The bimetallic Ag-CuO NPs had PDI values of 0.88, according to our findings. Based on the current values, the manufactured bimetallic nanoparticles demonstrated a reasonable range of polymorphism[85]. The results demonstrated that the HR-TEM imaging-derived particle estimations were smaller than the DLS analysis's average and prevalent sizes. According to the following reference, the hydrodynamic radius within the generated bimetallic Ag-CuO NPs and the water that surrounds layers are the causes of the significant sizes of the developed bimetallic NPs[86].

Because each measuring approach has its own set of principles and sensitivities, the technique used can have a substantial impact on the PSD data. Here are some important ways that this might occur such as sieve analysis[87], laser diffraction[88], DLS[89], microscopy[90], and sedimentation[91]. Every approach has advantages and disadvantages of its own, and the reported PSD values might be greatly impacted by the method used. Utilizing a variety of techniques is frequently advantageous in order to have a thorough comprehension of the particle size distribution distributions.

The Zeta potential of the resultant GA@Ag-CuO NPs was examined at a pH of 7.1 during the preparation, as shown in Fig. 3b. According to the current findings, during testing, the bimetallic Ag-CuO NPs contact's Zeta potential maintains a negative value at the substance's pH. Furthermore, the preparation's Zeta potential at standard medium (pH 7.1) was -27.5 ± 1.5 mV (they were performed in triplicate ($n = 3$)) as seen in Fig. 3b because of Gum Arabi's negative electrical charge. Table 1, summarized the different values of PSD, PDI, and zeta potential of the synthesized GA@Ag-CuO nanocomposite.

Figure 4 displays the XRD investigations for the produced NPs. This is the starting phase; the amorphous and crystal orientations in the NPs, respectively, show the resultant Ag NPs, CuO NPs, and Ag-CuO NPs. Figure 4 displayed the XRD diffraction peaks of Ag NPs. The peaks at $2\Theta = 38.32^{o}$, 44.58^{o}, 63.14^{o}, and 78.25^{o} matched Bragg's reflections (111), (200), (220), and (311), and they were associated with the standard card JCPDS-ICDD number 04-0783[92,93], on the other hand, the XRD of the synthesized CuO NPs showed clear peaks at $2\Theta = 31.15^{o}$, 36.78^{o}, 39.81^{o}, 51.88^{o}, 59.18^{o}, 67.89^{o}, and 70.21^{o}. Bragg's reflections (110), (002), (200), (202), (020), (022), and (220) were linked to these peaks, and they were accompanied by a special card with the JCPDS number 892,531[94].

Furthermore, the XRD diffraction peaks of Ag NPs and the outcomes of the produced bimetallic Ag-CuO NPs are shown in Fig. 4. The typical card JCPDS number 361,451, which corresponds to these peaks, is associated with the Bragg's reflections (111), (200), (220), and (311)[95].

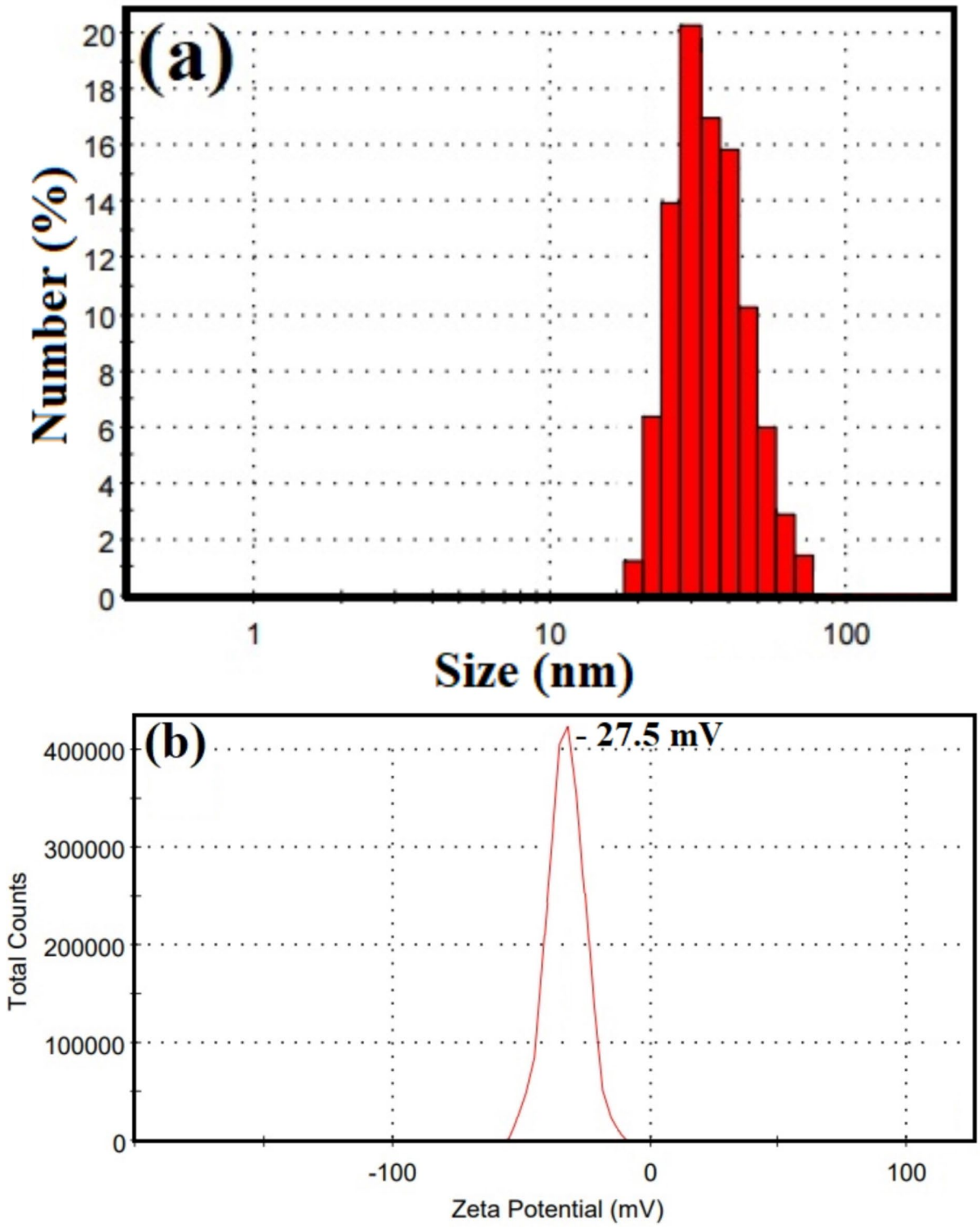

Fig. 3. Particle size distribution, and surface charge of the synthesized GA@Ag-CuO nanocomposite where (a) DLS analysis, and (b) Zeta potential (they were performed in triplicate ($n = 3$)).

Nanocomposite	PSD (nm)	PDI	Zeta potential (mV)
GA@Ag-CuO	55.42 ± 2.3	0.88	−27.5 ± 1.5

Table 1. PSD, PDI, and Zeta potential values of the synthesized GA@Ag-CuO nanocomposite.

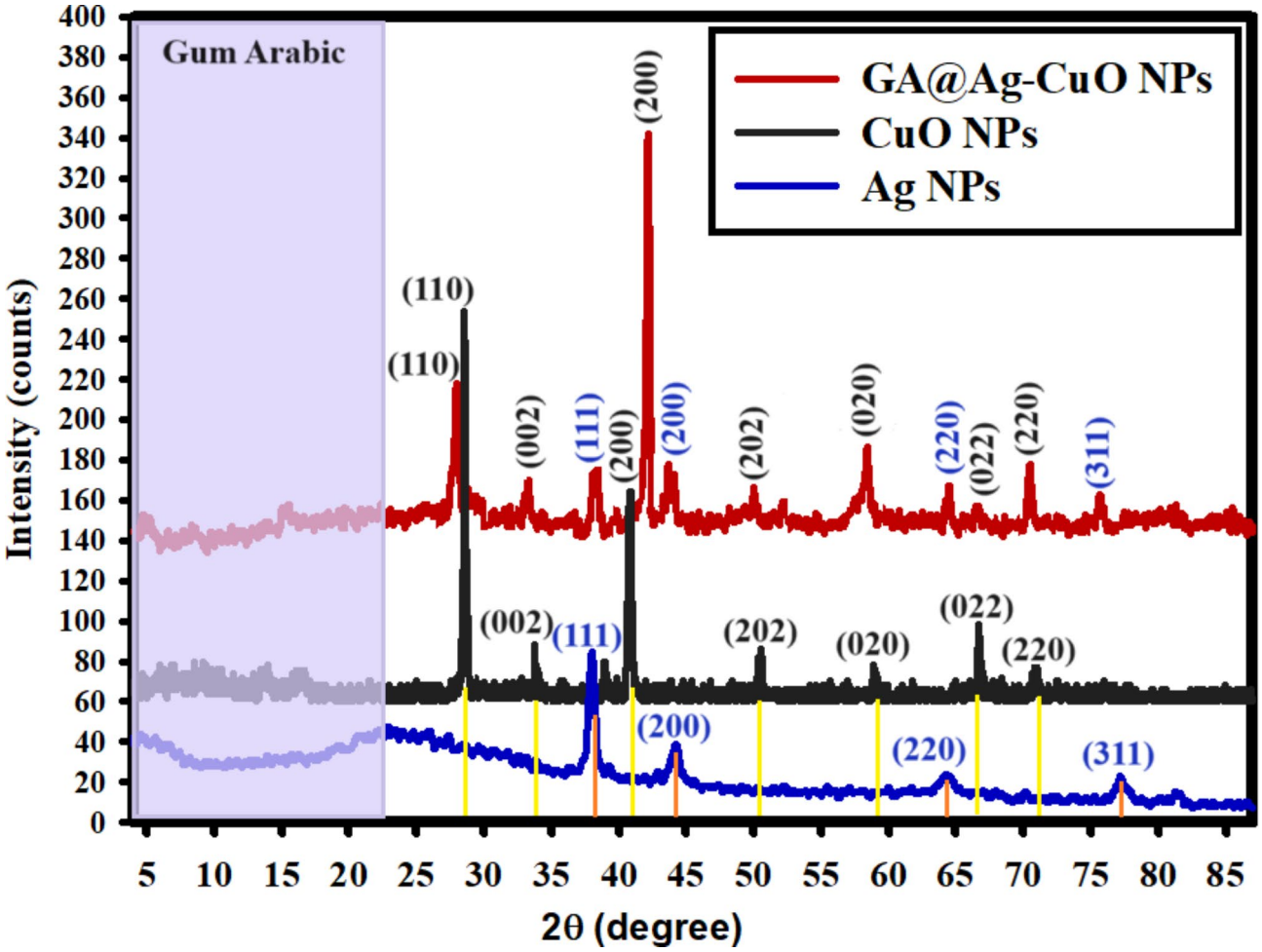

Fig. 4. XRD of the synthesized bimetallic Ag- CuO- NPs, CuO NPs, and Ag NPs.

The orientations of Bragg's reflections are (110), (002), (200), (202), (020), (022), and (220), as shown by the CuO NP diffraction peaks at 2Θ = 30.15°, 36.89°, 40.58°, 52.48°, 58.89°, 67.14°, and 71.78°. These peaks are supported by the JCPDS number 892,531 typical card[94].

Based on the available XRD data, the generated Ag-CuO NPs were created and had a face-centered (fcc) crystal structure (Fig. 4). The generated bimetallic NPs were highly crystalline and connected to gum Arabic heterogeneity, which improved their mobility in the solution to boost application, according to the XRD data[96].

The average crystallite size of the bimetallic Ag-CuO NPs was calculated using Williamson-Hall's Eq. (1)[97,98], and was found to be 20.25 nm.

$$\beta \cos\theta = \frac{k\lambda}{D}_{W-H} + 4\,\epsilon \sin\theta \quad (1)$$

Antimicrobial activity

Bimetallic nanoparticles have garnered considerable interest in antimicrobial research owing to their distinctive characteristics and heightened antibacterial efficacy in comparison to monometallic nanoparticles[99]. Bimetallic nanoparticles consist of two distinct metals, and their combined effects result in enhanced antibacterial effectiveness. The study involved the synthesis and evaluation of GA@Ag-CuO nanocomposite for their antibacterial efficacy against pathogenic bacterial and fungus species, as depicted in Fig. 5. The results demonstrated that the synthesized GA@Ag-CuO nanocomposite shown exceptional antibacterial activity against the tested strains of microorganisms. The synthesized GA@Ag-CuO nanocomposite showed antibacterial activity toward *S. epidermis*, *S. aureus*, *L. plantrum*, *S. typhimurium* where inhibition zones at concentration 1000 µg/ml were 29.0, 16.0, 25.0 and 18.66 mm respectively. The tested *S. epidermis* was the most sensitive among bacterial strains, while the tested *S. aureus* was the least sensitive to GA@Ag-CuO nanocomposite as shown Fig. 5A&B. Furthermore, MICs of GA@Ag-CuO nanocomposite toward all tested bacterial strains were determined as illustrated in Fig. 6. Results revealed that, MICs of GA@Ag-CuO nanocomposite were 15.62, 125, 31.25 and 125 µg/ml against *S. epidermis*, *S. aureus*, *L. plantrum*, *S. typhimurium* respectively. The antifungal

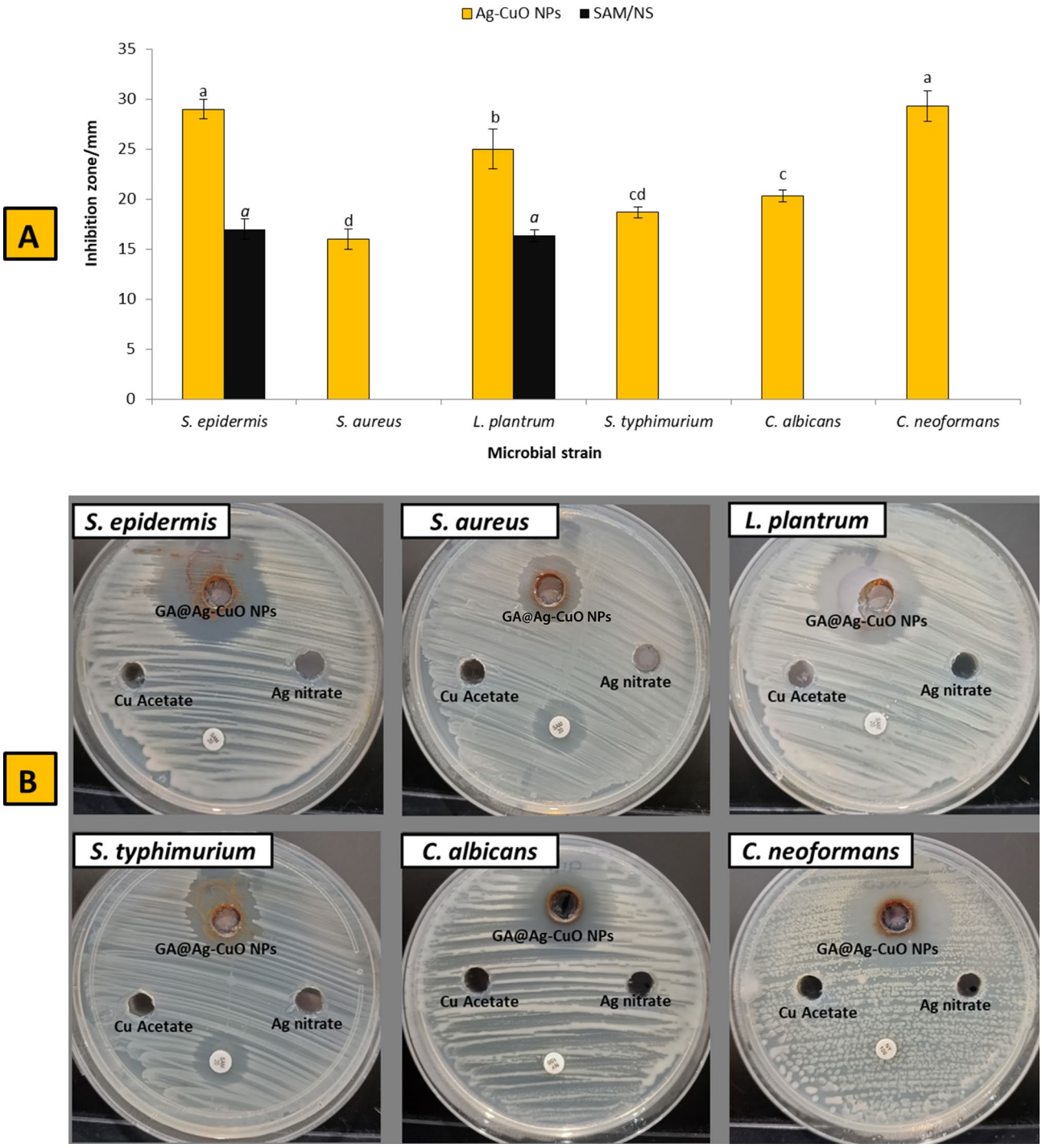

Fig. 5. Antimicrobial activity of GA@Ag-CuO nanocomposite, silver nitrate, copper acetate and SAM/NS against *S. epidermis*, *S. aureus*, *L. plantrum*, *S. typhimurium*, *C. albicans* and *C. neoformans* using agar well diffusion method (Agar well (**A**) & Inhibition zones (**B**)).

activity of GA@Ag-CuO nanocomposite was assessed against *C. albicans and C. neoformans*, as depicted in Fig. 5A&B.

The study found that the synthesized GA@Ag-CuO nanocomposite had significant antifungal efficacy against both *C. albicans and C. neoformans*, resulting in inhibition zones measuring 20.33 mm and 29.4 mm, respectively. In addition, MICs of Ag-CuO nanoparticles against *C. albicans* and *C. neoformans* were 62.5 and 15.62 µg/ml, respectively.

Prior research has established that bimetallic silver/copper nanoparticles possess antibacterial properties. Al-Haddad, Alzaabi[98] employed *Phoenix dactylifera* leaves for the eco-friendly synthesis of Cu-Ag bimetallic nanoparticles. Their study revealed that these nanoparticles have antibacterial properties against *B. subtilis* and

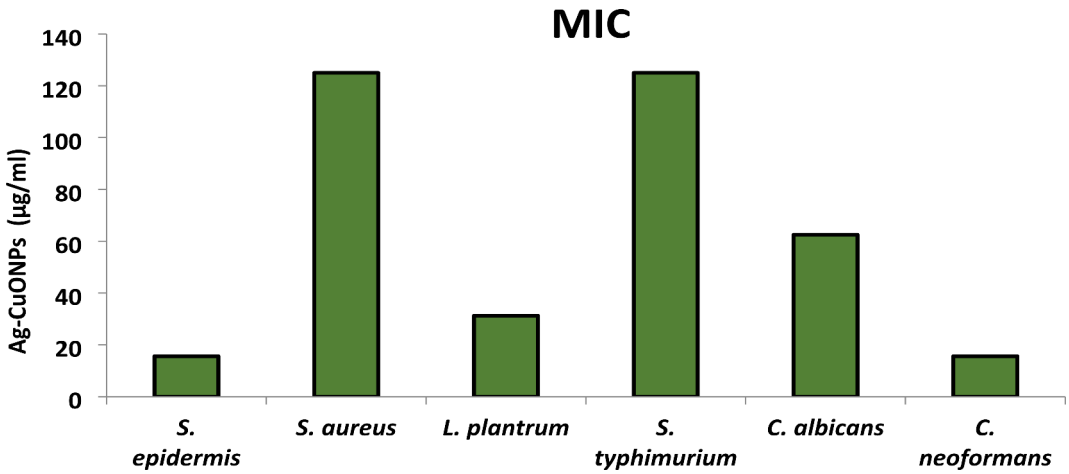

Fig. 6. Minimum inhibitory concentrations of GA@Ag-CuO nanocomposite toward tested bacterial and fungal strains.

E. coli. In addition, the Ag-Cu nanoparticles produced by the process of biosynthesis using *Aerva lanata* extract had antibacterial properties against both *S. aureus* and *Pseudomonas aeruginosa*. These nanoparticles were found to block the release of extracellular polysaccharides in a manner that depended on the dosage administered[55].

Furthermore, Bakina, Glazkova, Pervikov, Lozhkomoev, Rodkevich, Svarovskaya, Lerner, Naumova, Varnakova and Chjou[100] reported that Ag–Cu bimetallic nanoparticles displayed antibacterial activity of the nanoparticles against *E. coli* and *S. aureus* MRSA. Additionally, Ashishie, Inah and Ayi[101] verified that the Cu/Ag nanoparticles they created have antibacterial properties against *S. aureus*, resulting in a 21 mm inhibitory zone. Also, cotton fabrics based on Ag-Cu NPs were prepared and evaluated as antimicrobial agent, where results illustrated that these cotton fabrics have antimicrobial activity toward *E. coli*, *Enterobacter aerogenes*, *Proteus mirabilis*, *K. pneumonia* and *C. albicans* [102]. Paszkiewicz, Gołąbiewska, Rajski, Kowal, Sajdak and Zaleska-Medynska[103], reported that, Ag-Cu NPs showed promising antibacterial and antifungal activity toward *E. coli*, *S. aureus and C. albicans.*

Bimetallic Ag-CuO NPs have antibacterial action through multiple routes. The antibacterial activities of Ag-CuO NPs are attributed to the release of silver and copper ions when they come into contact with moisture or biological fluids (Scheme 2). Metal ions damage microbial cells through the mechanisms of destroying the cell membrane, interfering with DNA replication and transcription, and denaturing or affecting vital proteins (Scheme 2). In addition, Ag-CuO nanoparticles produce ROS that cause oxidative stress, resulting in cellular harm (Scheme 2)[57,104]. The combined actions of these many mechanisms contribute to the antibacterial properties of Ag-CuO NPs. Nevertheless, it is crucial to acknowledge that the precise methods can differ based on the characteristics of the nanoparticles and the microorganisms they are targeting.

Cytotoxicity of GA@Ag-CuO nanocomposite toward Wi 38 normal cell line

An essential component of preclinical research, assessing the cytotoxicity of compounds on normal cell lines is the determination of a compound's potential toxicity to healthy cells[105]. In this regard, determining the biosafety of compounds is regarded as the initial step toward their implementation in various disciplines. In the current study, the biosafety of GA@Ag-CuO nanocomposite was checked using Wi 38 normal cell line as shown in Fig. 7. Results revealed that, cell viability of Wi 38 cell line at conentrations 31.25, 62.5 and 125 µg/mL of GA@Ag-CuO nanocomposite were 99.3, 94.89 and 59.28% respectively. Also, IC_{50} of GA@Ag-CuO nanocomposite toward Wi 38 cell line was 154.2 µg/ml. Typically, if the IC50 is equal to or more than 90 µg/mL, the substance is categorised as non-cytotoxic[106]. Consequently, the synthesised GA@Ag-CuO nanocomposite are deemed to be safe for use. Therefore, we examined the safe concentrations and maximal non-toxic concentrations of this chemical to determine its anticancer activity.

Anticancer activity of GA@Ag-CuO nanocomposite

The synthesis of anticancer compounds is critical because it facilitates the identification and advancement of novel pharmaceuticals, which may result in significant advances in the treatment of cancer[107]. By synthesizing and modifying compounds, researchers can establish the structure-activity relationship, optimize drug properties, and overcome drug resistance, providing alternative options for patients[108].

In the current study, anticancer activity of GA@Ag-CuO nanocomposite was assessed toward MCF-7 and Hep-G2 cancerous cell lines. Results showed that, safe concentrations of GA@Ag-CuO nanocomposite exhibited promising anticancer activity toward both MCF-7 and Hep-G2 as shown in Fig. 8. Safe concentrations of GA@Ag-CuO nanocomposite (125 and 62.5 µg/mL) showed anticancer activity higher than 50% against both cancerous cell lines. Moreover, IC_{50} of GA@Ag-CuO nanocomposite toward MCF-7 and Hep-G2 was 26.11 and 59.5 µg/ml respectively. In compared to Taxol as positive control, IC50 of Taxol toward MCF-7 and Hep-G2 cell lines was 7.25 and 11.87 µg/ml.

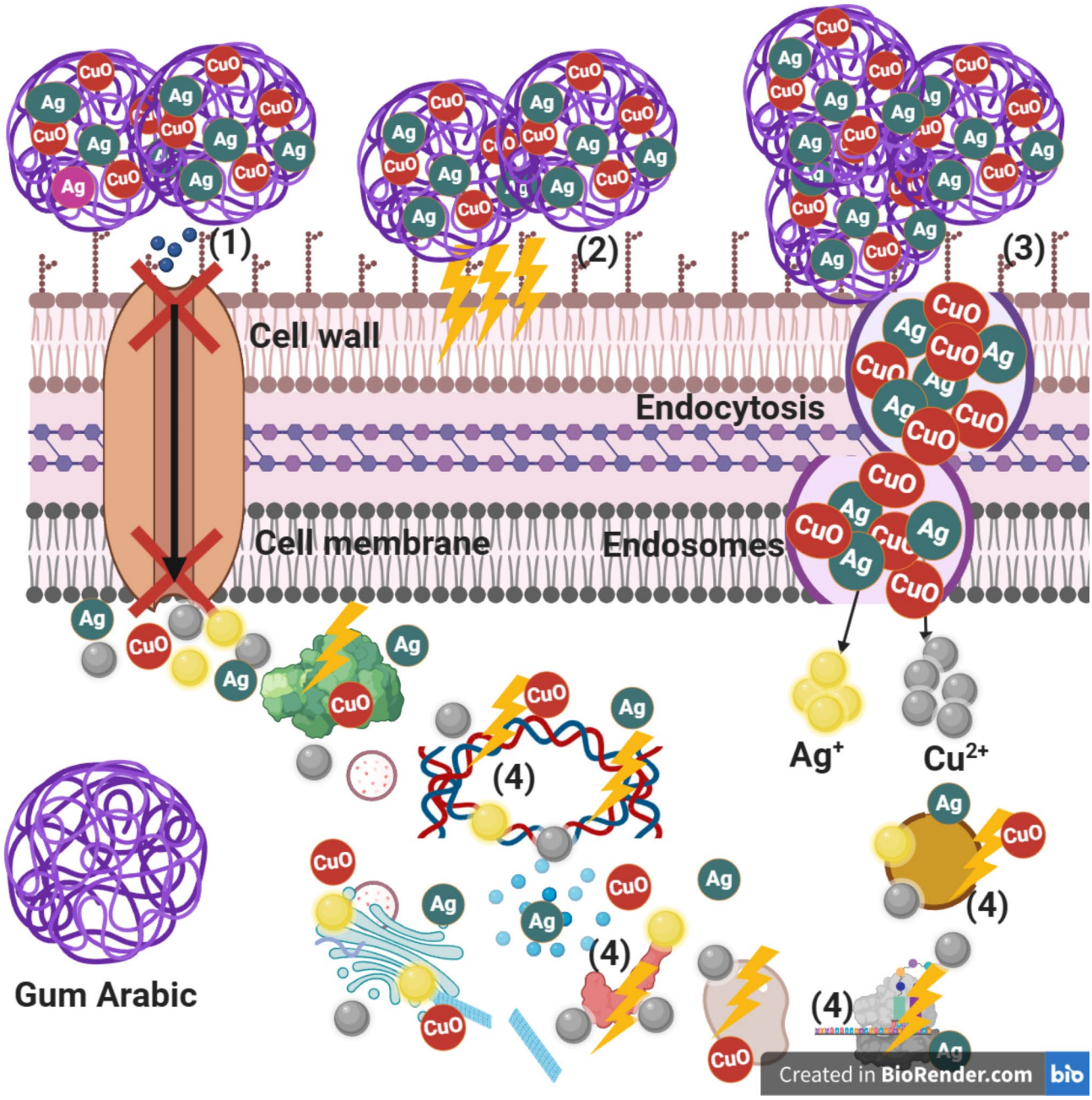

Scheme 2. The following reactions are indicative of the anticipated interaction between the produced GA@Ag-CuO nanocomposite and the bacterial cell (using Gram-positive bacteria as an example): Bimetallic nanoparticles affect bacterial cells in four primary ways: It does four things to the bacterial cell: (1) it prevents ions from entering the cell; (2) it creates and multiplies reactive oxygen species (ROS), which cause oxidative stress and may be a sign that the cell wall is beginning to weaken; (3) it adheres to the cell's exterior and results in membrane failure, endocytosis, the formation of endosomes, and altered transport potential; and (4) it enters the cell and interacts with organelles, such as DNA, to change their functions and cause bacterial cell lysis. In the cytoplasm and layer, where the presence of a proton motive force may cause the pH to drop below 3.0 and induce the discharge of Ag and Cu ions, GA@Ag-CuO nanocomposite may also function as a carrier to effectively release Ag and Cu ions. **The scheme was designed by BioRender.com**.

Nanometals have received much attention due to their high efficacy as antimicrobial as well as anticancer agents[28,109,110]. Yang, Zhang, Velu, Liu and Vijayalakshmi[111], used *Leucas aspera* aqueous leaf extract for biosynthesis Ag-Cu NPs, these bimetallic nanoparticles showed promising anticancer activity against alveolar cancer cell line. The Ag–Cu NPs which phyto-fabricated by *Aerva lanata* extract exhibit potent cytotoxic activity against cancerous HeLa cell lines, with an inhibitory concentration (IC50) of 17.63 µg/ml[55].

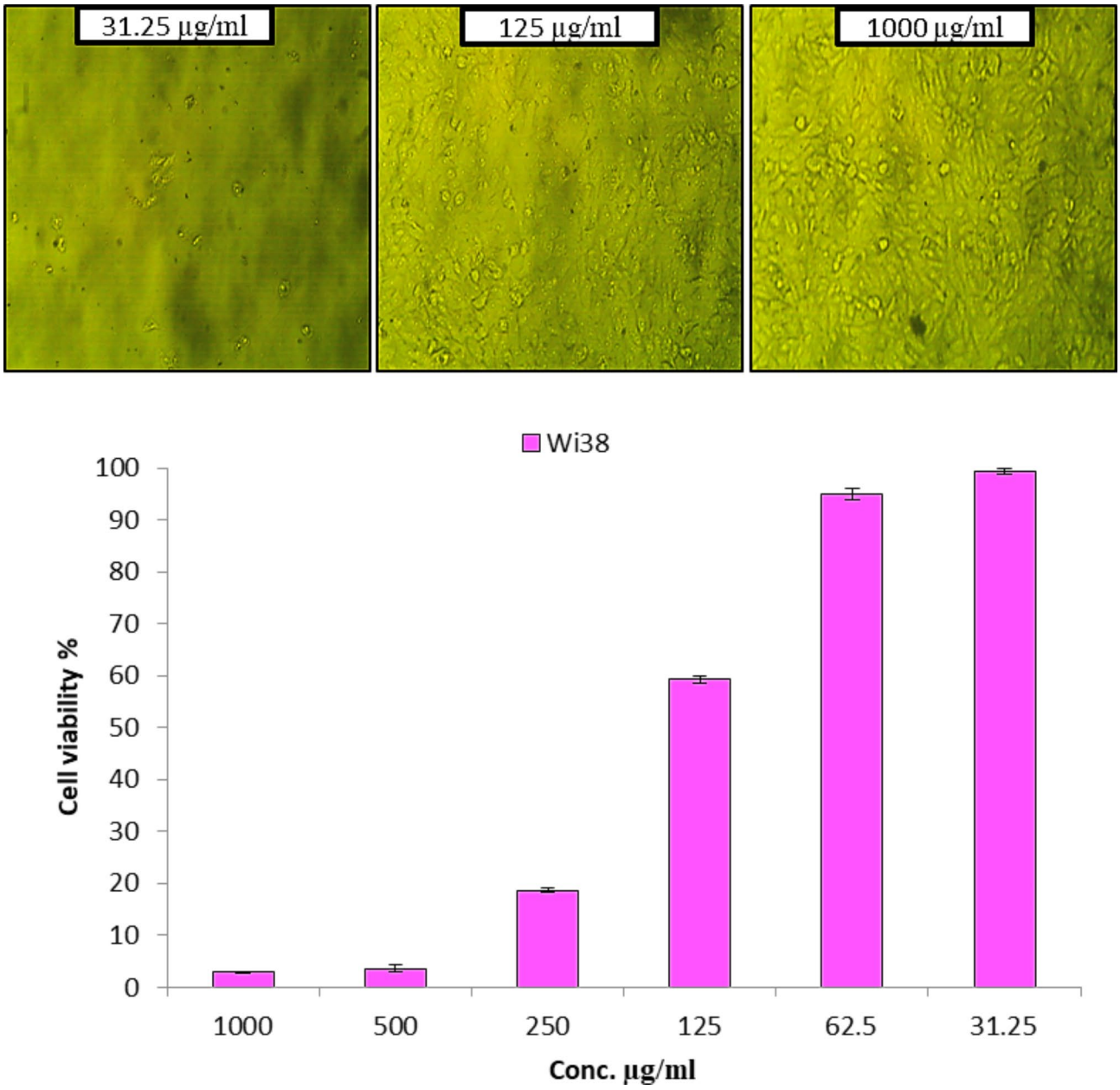

Fig. 7. Cell viability of Wi 38 cell line at different concentrations of GA@Ag-CuO nanocomposite.

In their study, Banik, Patra, Dutta, Mukherjee and Basu[112] found that bimetallic Cu-Ag nanoparticles (NPs) exhibited a higher level of toxicity towards cancer cells compared to normal cells. The dose of the NPs, which ranged from 4 to 5 µg ml^{-1}, is responsible for killing approximately 75% of the various human cancer cell lines, including HepG2 (for liver cancer), A549 (for lung cancer), and AGS (for stomach cancer). However, the dose of the NPs was only sufficient to kill approximately 22.5% of the normal cell lines, specifically WRL68 (for liver) and WI38 (for lung cancer). Ag-Cu nanoparticles, which are bimetallic, exhibit significant anticancer action through a variety of different routes.

These nanoparticles combine the anticancer characteristics of silver and copper, which are both known to be effective against cancer. Ag-Cu nanoparticles have the ability to result in oxidative stress by means of the production of ROS, which in turn can result in DNA damage, cellular death, and the prevention of cancer cell proliferation. Furthermore, Ag-Cu NPs can interfere with cellular signaling pathways, inhibit angiogenesis, and modulate the tumor microenvironment. The synergistic effects of silver and copper in these bimetallic nanoparticles make them promising candidates for anticancer therapeutics, offering potential benefits in cancer treatment and control[113].

The diverse array of mechanisms by which bimetallic nanoparticles exert their anticancer effects underscores their potential as highly promising therapeutic candidates for cancer.

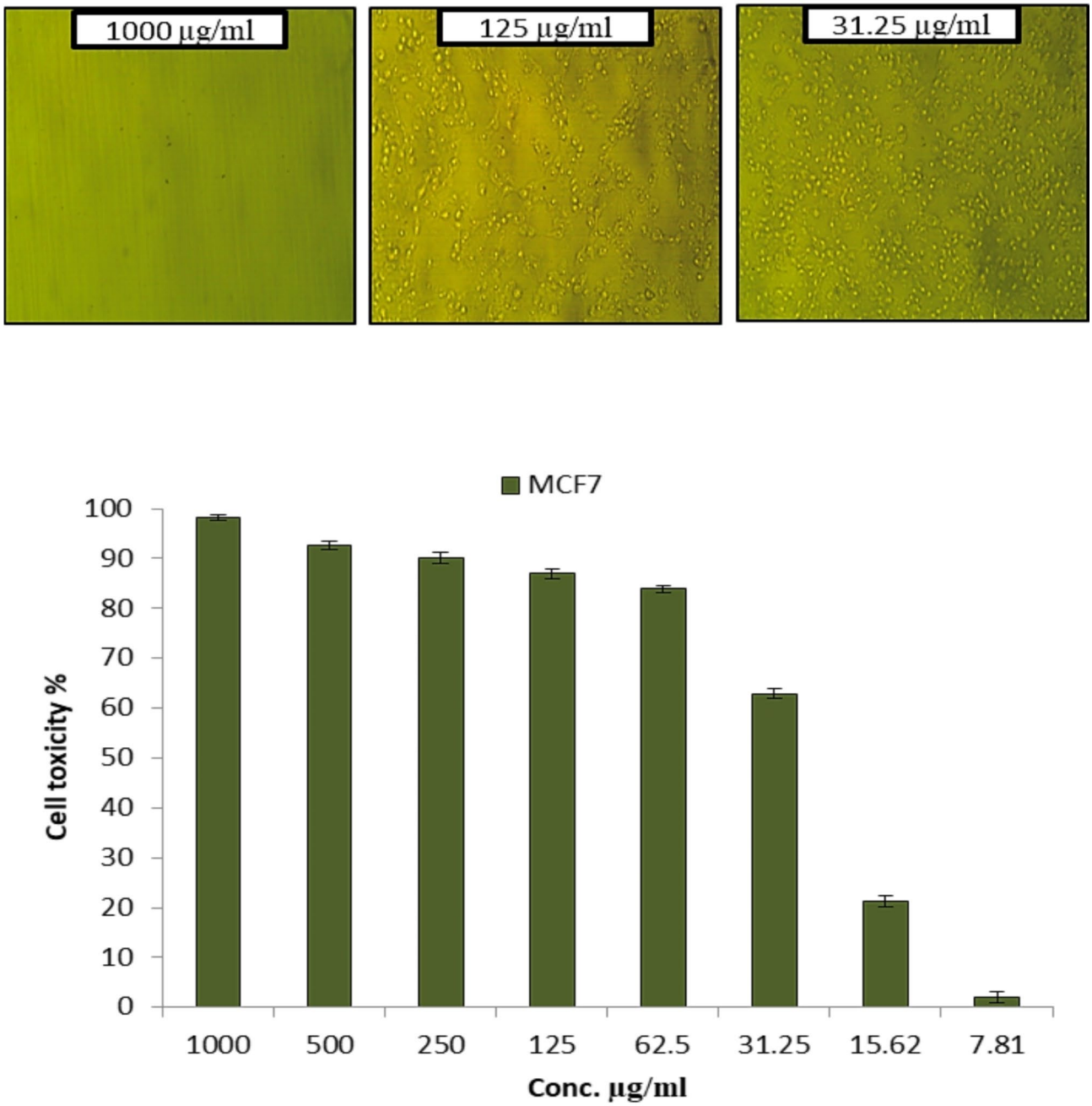

Fig. 8. Anticancer activity of GA@Ag-CuO nanocomposite toward two cancerous cell lines MCF-7 (Top) and Hep-G2 (Bottom).

Conclusion

In the current study, a novel GA@Ag-CuO nanocomposite was synthesized and thoroughly characterized. The biosafety assessment of this nanocomposite toward the Wi 38 normal cell line showed that it was safe, with an IC50 value of 154.2 µg/ml. The antimicrobial results confirmed that the synthesized GA@Ag-CuO nanocomposite exhibited promising antibacterial activity against *S. epidermis*, *S. aureus*, *L. plantrum*, *and S. typhimurium*, with MIC values ranging from 15.62 to 125 µg/ml. Additionally, the nanocomposite displayed antifungal activity against *C. albicans* and *C. neoformans*, with MIC values of 62.5 and 15.62 µg/ml, respectively. Furthermore, the GA@Ag-CuO nanocomposite demonstrated significant anticancer activity, with IC50 values of 26.11 and 59.5 µg/ml against MCF-7 and Hep-G2 cell lines, respectively. However, the study was limited in scope, focusing on a small set of microorganisms and cell lines, and lacked detailed mechanistic insights. Future research should delve into the mechanism of action, conduct in vivo studies, and optimize the synthesis process

for enhanced efficacy. If successful, this research could lead to the development of novel therapeutic agents for various diseases, contributing to the fight against antibiotic resistance pathogenic microbes and cancer cells.

Data availability

The datasets used and analyzed during the current study are available from the corresponding author on reasonable request.

Received: 11 July 2024; Accepted: 14 October 2024
Published online: 03 January 2025

References

1. Crum-Cianflone, N. F. Bacterial, fungal, parasitic, and viral myositis. *Clin. Microbiol. Rev.* **21** (3), 473–494 (2008).
2. Khezerlou, A., Alizadeh-Sani, M., Azizi-Lalabadi, M. & Ehsani, A. Nanoparticles and their antimicrobial properties against pathogens including bacteria, fungi, parasites and viruses. *Microb. Pathog.* **123**, 505–526 (2018).
3. Kantele, A., Chickering, K., Vapalahti, O. & Rimoin, A. Emerging diseases—the monkeypox epidemic in the Democratic Republic of the Congo. *Clin. Microbiol. Infect.* **22** (8), 658–659 (2016).
4. Bloom, D. E. & Cadarette, D. Infectious disease threats in the twenty-first century: strengthening the global response. *Front. Immunol.* **10**, 549 (2019).
5. Coates, A., Hu, Y., Bax, R. & Page, C. The future challenges facing the development of new antimicrobial drugs. *Nat. Rev. Drug Discovery*. **1** (11), 895–910 (2002).
6. Ventola, C. L. The antibiotic resistance crisis: part 1: causes and threats. *Pharm. Ther.* **40** (4), 277 (2015).
7. Aljeldah, M. M. Antimicrobial resistance and its spread is a global threat. *Antibiotics*. **11** (8), 1082 (2022).
8. Moo, C. L. et al. Mechanisms of antimicrobial resistance (AMR) and alternative approaches to overcome AMR. *Curr. Drug Discov. Technol.* **17** (4), 430–447 (2020).
9. El-Sayyad, G. S. The need for smart bimetallic nanoparticles in the battle against pathogenic multi-drug resistant bacteria: a brief communication. *Discover Bacteria*. **1** (1), 2 (2024).
10. Muteeb, G. & Rehman, M. T. Origin of antibiotics and antibiotic resistance, and their impacts on Drug Development: a narrative review, **16**(11) (2023).
11. Prestinaci, F., Pezzotti, P. & Pantosti, A. Antimicrobial resistance: a global multifaceted phenomenon. *Pathog Glob Health*. **109** (7), 309–318 (2015).
12. Holohan, C., Van Schaeybroeck, S., Longley, D. B. & Johnston, P. G. Cancer drug resistance: an evolving paradigm, Nature reviews. *Cancer*. **13** (10), 714–726 (2013).
13. Zahreddine, H. & Borden, K. L. Mechanisms and insights into drug resistance in cancer. *Front. Pharmacol.* **4**, 28 (2013).
14. Anand, U. et al. Cancer chemotherapy and beyond: current status, drug candidates, associated risks and progress in targeted therapeutics. *Genes Dis.* **10** (4), 1367–1401 (2023).
15. Shuel, S. L. Targeted cancer therapies: clinical pearls for primary care. *Can. Family Physician Medecin De Famille Canadien*. **68** (7), 515–518 (2022).
16. Dallavalle, S. et al. Improvement of conventional anti-cancer drugs as new tools against multidrug resistant tumors. *Drug Resist. Updates*. **50**, 100682 (2020).
17. Voulgari, A. & Pintzas, A. Epithelial–mesenchymal transition in cancer metastasis: mechanisms, markers and strategies to overcome drug resistance in the clinic. *Biochim. et Biophys. Acta (BBA)-Reviews Cancer*. **1796(2)**, 75–90 (2009).
18. Pao, W. et al. Acquired resistance of lung adenocarcinomas to gefitinib or erlotinib is associated with a second mutation in the EGFR kinase domain. *PLoS Med.* **2** (3), e73 (2005).
19. Eid, A. M. et al. Hassan, harnessing bacterial endophytes for promotion of plant growth and biotechnological applications: an overview. *Plants*. **10** (5), 935 (2021).
20. Rajwade, J. M., Chikte, R. & Paknikar, K. Nanomaterials: new weapons in a crusade against phytopathogens. *Appl. Microbiol. Biotechnol.* **104** (4), 1437–1461 (2020).
21. Fu, L., Wang, Z., Dhankher, O. P. & Xing, B. Nanotechnology as a new sustainable approach for controlling crop diseases and increasing agricultural production. *J. Exp. Bot.* **71** (2), 507–519 (2020).
22. Tyagi, P. K. Production of metal nanoparticles from biological resources. *Int. J. Curr. Microbiol. Appl. Sci.* **5** (3), 548–558 (2016).
23. Abd Elkodous, M. et al. Recent advances in waste-recycled nanomaterials for biomedical applications: Waste-to-wealth. *Nanatechnol. Reviews*. **10** (1), 1662–1739 (2021).
24. Kamaruzaman, N. H. et al. Applicability of bio-synthesized nanoparticles in fungal secondary metabolites products and plant extracts for eliminating antibiotic-resistant bacteria risks in non-clinical environments. *Environ. Res.* **209**, 112831 (2022).
25. Hashem, A. H. et al. Unveiling Antimicrobial and Insecticidal activities of Biosynthesized Selenium nanoparticles using Prickly Pear Peel Waste. *J. Funct. Biomaterials*. **13** (3), 112 (2022).
26. Ali, O. M., Hasanin, M. S., Suleiman, W. B., Helal, E. E. H. & Hashem, A. H. Green biosynthesis of titanium dioxide quantum dots using watermelon peel waste: antimicrobial, antioxidant, and anticancer activities, Biomass Conversion and Biorefinery (2022).
27. Saied, E. et al. Mycosynthesis of Hematite (α-Fe2O3) Nanoparticles Using Aspergillus niger andTheir Antimicrobial and Photocatalytic Activities. *Bioengineering* **9**(8), 397 (2022).
28. Saied, E. et al. Photocatalytic and antimicrobial activities of biosynthesized silver nanoparticles using cytobacillus firmus. *Life*. **12** (9), 1331 (2022).
29. Hashem, A. H. et al. Antifungal activity of Biosynthesized Silver nanoparticles (AgNPs) against Aspergilli Causing aspergillosis: Ultrastructure Study. *J. Funct. Biomaterials*. **13** (4), 242 (2022).
30. Gaur, M., Misra, C., Bajpayee, A. K. & Bhardwaj, A. K. Recent advances in agriculture waste for nanomaterial production, Green and sustainable approaches using wastes for the production of multifunctional nanomaterials 331–344. (2024).
31. Narwal, N. et al. Sustainable advances in the synthesis of waste-derived value-added metal nanoparticles and their applications, Green and Sustainable Approaches Using Wastes for the Production of Multifunctional Nanomaterials, Elsevier2024, pp. 17–33 .
32. Chauhan, S. B., Saxena, S. & Bhardwaj, A. K. Industrial wastes and their suitability for the synthesis of nanomaterials, Green and Sustainable Approaches Using Wastes for the Production of Multifunctional Nanomaterials, Elsevier2024, pp. 103–115.
33. Bhardwaj, A. K. & Naraian, R. Cyanobacteria as biochemical energy source for the synthesis of inorganic nanoparticles, mechanism and potential applications: a review. *3 Biotech.* **11** (10), 445 (2021).
34. Naseri, M. G., Saion, E. B., Ahangar, H. A. & Shaari, A. H. Fabrication, characterization, and magnetic properties of copper ferrite nanoparticles prepared by a simple, thermal-treatment method. *Mater. Res. Bull.* **48** (4), 1439–1446 (2013).
35. El-Batal, A. I. et al. Gum arabic polymer-stabilized and Gamma rays-assisted synthesis of bimetallic silver-gold nanoparticles: powerful antimicrobial and antibiofilm activities against pathogenic microbes isolated from diabetic foot patients. *Int. J. Biol. Macromol.* **165**, 169–186 (2020).
36. Chawla, P. et al. Gum arabic capped copper nanoparticles: synthesis, characterization, and applications. *Int. J. Biol. Macromol.* (2020).

37. Govindasamy, G. A., Mydin, R. B. S. M. N., Gadaime, N. K. R. & Sreekantan, S. Phytochemicals, Biodegradation, Cytocompatibility and Wound Healing profiles of Chitosan Film embedded Green Synthesized Antibacterial ZnO/CuO Nanocomposite. *J. Polym. Environ.* **31** (10), 4393–4409 (2023).
38. Khan, I., Saeed, K. & Khan, I. Nanoparticles: Properties, applications and toxicities. *Arab. J. Chem.Bold">12* (7), 908–931 (2019).
39. Govindasamy, G. A., Mydin, R. B. S. M. N., Effendy, W. N. F. W. E. & Sreekantan, S. Novel dual-ionic ZnO/CuO embedded in porous chitosan biopolymer for wound dressing application: Physicochemical, bactericidal, cytocompatibility and wound healing profiles. *Mater. Today Commun.* **33**, 104545 (2022).
40. Govindasamy, G. A., Mydin, R. B. S. M. N., Sreekantan, S. & Harun, N. H. Compositions and antimicrobial properties of binary ZnO–CuO nanocomposites encapsulated calcium and carbon from Calotropis gigantea targeted for skin pathogens. *Sci. Rep.* **11** (1), 99 (2021).
41. Govindasamy, G. A. et al. *Effect of Compositions and Heat Treatments of Polypropylene/PP-g-MAH/CuO-TiO2 Composites on Thermal* (Crystallization and Antimicrobial Properties, 2024).
42. Govindasamy, G. A., Mydin, R. B. S., Sreekantan, S. & Harun, N. H. Effect of calcination temperature on physicochemical and antimicrobial properties of green synthesised ZnO/C/Ca nanocomposites using Calotropis gigantea leaves. *Adv. Nat. Sci. NanoSci. NanoTechnol.* **12** (1), 015013 (2021).
43. GovindasamyG.A. et al. Composition-dependent Physicochemical and Bactericidal properties of Dual Cu-TiO2 Nanoparticles Incorporated in Polypropylene. *BioNanoScience*. **14** (2), 770–782 (2024).
44. Govindasamy, G. A., Mydin, R. B. S. M. N., Harun, N. H., Effendy, W. N. F. W. E. & Sreekantan, S. Giant milkweed plant-based copper oxide nanoparticles for wound dressing application: physicochemical, bactericidal and cytocompatibility profiles. *Chem. Pap.* **77** (2), 1181–1200 (2023).
45. Elakraa, A. A., Salem, S. S., El-Sayyad, G. S. & Attia, M. S. Cefotaxime incorporated bimetallic silver-selenium nanoparticles: promising antimicrobial synergism, antibiofilm activity, and bacterial membrane leakage reaction mechanism. *RSC Adv.* **12** (41), 26603–26619 (2022).
46. Hashem, A. H. & El-Sayyad, G. S. Antimicrobial and anticancer activities of biosynthesized bimetallic silver-zinc oxide nanoparticles (Ag-ZnO NPs) using pomegranate peel extract, Biomass Conversion and Biorefinery (2023).
47. Gaber, S. E., Hashem, A. H., El-Sayyad, G. S. & Attia, M. S. Antifungal activity of myco-synthesized bimetallic ZnO-CuO nanoparticles against fungal plant pathogen Fusarium oxysporum, Biomass Conversion and Biorefinery (2023).
48. El-Behery, R. R., El-Sayed, E. S. R. & El-Sayyad, G. S. Gamma rays-assisted bacterial synthesis of bimetallic silver-selenium nanoparticles: powerful antimicrobial, antibiofilm, antioxidant, and photocatalytic activities. *BMC Microbiol.* **23** (1), 224 (2023).
49. El-Batal, A. I. et al. Gum arabic-assisted biomass synthesis of bimetallic ZnO-CuO nanoparticles using gamma rays for controlling potato post-harvest tuber rots-causing Alternaria solani: towards improving food safety. *Biomass Convers. Biorefinery* (2023).
50. Attia, M. S. et al. Protective role of Mycosynthesized Bimetallic ZnO-CuO nanoparticles as therapeutic nutrients to enhance the resistance of Vicia faba against Fusarium Wilt Disease. *Agronomy*. **13** (11), 2725 (2023).
51. Elkhodary, B. H., Attia, M. S., El-Sayyad, G. S. & Salem, M. S. Effectiveness of bimetallic ZnO-B2O3 nanoparticles produced by Streptomyces gancidicus as prospective antifungal agents and therapeutic nutrients to enhance pea plant immunity against damping off-causing Pythium irregulare: in vivo and in vitro investigations. *Biomass Convers. Biorefinery* (2023).
52. Hashem, A. H. et al. Watermelon rind mediated biosynthesis of bimetallic selenium-silver nanoparticles: characterization, Antimicrobial and Anticancer activities. *Plants*. **12** (18), 3288 (2023).
53. Mostafa, H. Y., El-Sayyad, G. S., Nada, H. G., Ellethy, R. A. & Zaki, E. G. Promising antimicrobial and antibiofilm activities of Orobanche Aegyptiaca extract-mediated bimetallic silver-selenium nanoparticles synthesis: Effect of UV-exposure, bacterial membrane leakage reaction mechanism, and kinetic study. *Arch. Biochem. Biophys.* **736**, 109539 (2023).
54. El-Batal, A. I. et al. Gum arabic assisted the biomass synthesis of bimetallic silver copper oxide nanoparticles using gamma-rays for improving bacterial and viral wound healing: promising antimicrobial activity against foot and mouth disease. *Int. J. Biol. Macromol.* **262**, 130010 (2024).
55. Thirumoorthy, G. et al. Veerappa Lakshmaiah, Phytofabricated bimetallic synthesis of silver-copper nanoparticles using Aerva lanata extract to evaluate their potential cytotoxic and antimicrobial activities. *Sci. Rep.* **14** (1), 1270 (2024).
56. Abdul Hak, A., Zedan, H. H., El-Mahallawy, H. A., El-Sayyad, G. S. & Zafer, M. M. In Vivo and in Vitro activity of colistin-conjugated bimetallic silver-copper oxide nanoparticles against Pandrug-resistant Pseudomonas aeruginosa. *BMC Microbiol.* **24** (1), 213 (2024).
57. Hao, Z. et al. Synergistic antibacterial mechanism of silver-copper bimetallic nanoparticles. *Front. Bioeng. Biotechnol.* **11**, 1337543 (2024).
58. Daimari, J., Basumatary, S. & Deka, A. K. Bimetallic nanoparticles from coinage metals (Cu, Ag, au) and its biomedical applications: a review. *Nano-Structures Nano-Objects*. **39**, 101247 (2024).
59. Saad, A. M. et al. Polyphenolic extracts from pomegranate and watermelon wastes as substrate to fabricate sustainable silver nanoparticles with larvicidal effect against Spodoptera Littoralis. *Saudi J. Biol. Sci.* **28** (10), 5674–5683 (2021).
60. Said, A., Abu-Elghait, M., Atta, H. M. & Salem, S. S. Antibacterial activity of green synthesized silver nanoparticles using lawsonia inermis against common pathogens from urinary tract infection. *Appl. Biochem. Biotechnol.* 1–14. (2023).
61. N.C.f.C.L & Standards Reference method for broth dilution antifungal susceptibility testing of yeasts, National Committee for Clinical Laboratory Standards Wayne, PA, (2002).
62. Valgas, C., Souza, S. M. D., Smânia, E. & Smânia, A. Screening methods to determine antibacterial activity of natural products. *Brazilian J. Microbiol.* **38**, 369–380 (2007).
63. Hashem, A. H., Khalil, A. M. A., Reyad, A. M. & Salem, S. S. Biomedical Applications of Mycosynthesized Selenium nanoparticles using Penicillium Expansum ATTC 36200. *Biol. Trace Elem. Res.* (2021).
64. Dacrory, S., Hashem, A. H. & Hasanin, M. Synthesis of cellulose based amino acid functionalized nano-biocomplex: characterization, antifungal activity, molecular docking and hemocompatibility, Environmental Nanotechnology. *Monit. Manage.* **15**, 100453 (2021).
65. Van de Loosdrecht, A., Beelen, R., Ossenkoppele, Broekhoven, M. & Langenhuijsen, M. A tetrazolium-based colorimetric MTT assay to quantitate human monocyte mediated cytotoxicity against leukemic cells from cell lines and patients with acute myeloid leukemia. *J. Immunol. Methods*. **174** (1–2), 311–320 (1994).
66. Sui, M., Kunwar, S., Pandey, P. & Lee, J. Strongly confined localized surface plasmon resonance (LSPR) bands of pt, AgPt, AgAuPt nanoparticles. *Sci. Rep.* **9** (1), 1–14 (2019).
67. Mohamed, A. A., Abu-Elghait, M., Ahmed, N. E. & Salem, S. S. Eco-friendly mycogenic synthesis of ZnO and CuO nanoparticles for in vitro antibacterial, antibiofilm, and antifungal applications. *Biol. Trace Elem. Res.* **199**, 2788–2799 (2021).
68. Barzinjy, A. A. & Azeez, H. H. Green synthesis and characterization of zinc oxide nanoparticles using Eucalyptus globulus Labill. Leaf extract and zinc nitrate hexahydrate salt. *SN Appl. Sci.* **2** (5), 991 (2020).
69. Rani, H. et al. In-vitro catalytic, antimicrobial and antioxidant activities of bioengineered copper quantum dots using Mangifera indica (L.) leaf extract. *Mater. Chem. Phys.* **239**, 122052 (2020).
70. Fouda, A., Salem, S. S., Wassel, A. R., Hamza, M. F. & Shaheen, T. I. Optimization of green biosynthesized visible light active CuO/ZnO nano-photocatalysts for the degradation of organic methylene blue dye. *Heliyon*. **6** (9), e04896 (2020).
71. Munir, R. et al. Biosynthesis of Leucaena Leucocephala leaf mediated ZnO, CuO, MnO2, and MgO based nano-adsorbents for reactive Golden Yellow-145 (RY-145) and Direct Red-31 (DR-31) dye removal from textile wastewater to reuse in agricultural purpose. *Sep. Purif. Technol.* **306**, 122527 (2023).

72. Badawy, A. A., Abdelfattah, N. A., Salem, S. S., Awad, M. F. & Fouda, A. Efficacy assessment of biosynthesized copper oxide nanoparticles (cuo-nps) on stored grain insects and their impacts on morphological and physiological traits of wheat (triticum aestivum l.) plant. *Biology*. **10** (3), 233 (2021).
73. Kelly, K. L., Coronado, E., Zhao, L. L. & Schatz, G. C. *The Optical Properties of Metal Nanoparticles: The Influence of size, Shape, and Dielectric Environment* (ACS, 2003).
74. Prasad, K. S. & Selvaraj, K. Biogenic synthesis of selenium nanoparticles and their effect on as (III)-induced toxicity on human lymphocytes. *Biol. Trace Elem. Res.* **157** (3), 275–283 (2014).
75. Khazaei, K. M., Jafari, S., Ghorbani, M. & Kakhki, A. H. Application of maltodextrin and gum arabic in microencapsulation of saffron petal's anthocyanins and evaluating their storage stability and color. *Carbohydr. Polym.* **105**, 57–62 (2014).
76. Moschakis, T., Murray, B. S. & Biliaderis, C. G. Modifications in stability and structure of whey protein-coated o/w emulsions by interacting chitosan and gum arabic mixed dispersions. *Food Hydrocoll.* **24** (1), 8–17 (2010).
77. Sukhotu, R. et al. Changes in physiochemical properties and stability of peanut oil body emulsions by applying gum arabic. *LWT-Food Sci. Technol.* **68**, 432–438 (2016).
78. El-Batal, A. I., Balabel, N. M., Attia, M. S. & El-Sayyad, G. S. Antibacterial and Antibiofilm potential of mono-dispersed stable copper Oxide nanoparticles-Streptomycin Nano-drug: implications for some Potato Plant Bacterial Pathogen Treatment. *J. Cluster Sci.* (2019).
79. Ashour, A. et al. Antimicrobial activity of metal-substituted cobalt ferrite nanoparticles synthesized by sol–gel technique, Particuology (2018).
80. Lawrie, A., Albanyan, A., Cardigan, R., Mackie, I. & Harrison, P. Microparticle sizing by dynamic light scattering in fresh-frozen plasma. *Vox Sang.* **96** (3), 206–212 (2009).
81. Monika, P. et al. Recent advances in pomegranate peel extract mediated nanoparticles for clinical and biomedical applications. *Biotechnol. Genet. Eng. Rev.* 1–29. (2022).
82. Mohsin, M. et al. An Insight into the Coating Behavior of Bimetallic Silver and Gold Core-Shell Nanoparticles, PLASMONICS (2020).
83. Castro-Longoria, E., Vilchis-Nestor, A. R. & Avalos-Borja, M. Biosynthesis of silver, gold and bimetallic nanoparticles using the filamentous fungus Neurospora Crassa. *Colloids Surf., B.* **83** (1), 42–48 (2011).
84. Nissen, M. et al. Nanoparticle tracking in single-antiresonant-element Fiber for high-Precision size distribution analysis of Mono-and polydisperse samples. *Small*. **18** (38), 2202024 (2022).
85. Salem, S. S. Bio-fabrication of selenium nanoparticles using Baker's yeast extract and its antimicrobial efficacy on food borne pathogens. *Appl. Biochem. Biotechnol.* **194** (5), 1898–1910 (2022).
86. Souza, T. G., Ciminelli, V. S. & Mohallem, N. D. S. A comparison of TEM and DLS methods to characterize size distribution of ceramic nanoparticles, Journal of Physics: Conference Series, IOP Publishing, p. 012039. (2016).
87. Magzoub, M. I. et al. An investigation of the swelling kinetics of bentonite systems using particle size analysis. *J. Dispers. Sci. Technol.* **41** (6), 817–827 (2020).
88. Shulkin, V. & Strukov, A. Y. Particle-size analysis of modern bottom sediments by the laser diffraction and sieve methods. *Russian J. Pac. Geol.* **14**, 378–386 (2020).
89. Farkas, N. & Kramar, J. A. Dynamic light scattering distributions by any means. *J. Nanopart. Res.* **23** (5), 120 (2021).
90. FalsafiS.R., Rostamabadi, H., Assadpour, E. & Jafari, S. M. Morphology and microstructural analysis of bioactive-loaded micro/nanocarriers via microscopy techniques; CLSM/SEM/TEM/AFM. *Adv. Colloid Interface Sci.* **280**, 102166 (2020).
91. Samal, S. Effect of shape and size of filler particle on the aggregation and sedimentation behavior of the polymer composite. *Powder Technol.* **366**, 43–51 (2020).
92. Jyoti, K., Baunthiyal, M. & Singh, A. Characterization of silver nanoparticles synthesized using Urtica dioica Linn. Leaves and their synergistic effects with antibiotics. *J. Radiation Res. Appl. Sci.* **9** (3), 217–227 (2016).
93. El-Behery, R. R., El-Sayed, E. S. R. & El-Sayyad, G. S. Gamma rays-assisted bacterial synthesis of bimetallic silver-selenium nanoparticles: powerful antimicrobial, antibiofilm, antioxidant, and photocatalytic activities. *BMC Microbiol.* **23** (1), 1–18 (2023).
94. Siddiquee, M. A. et al. Biogenic synthesis, in-vitro cytotoxicity, esterase activity and interaction studies of copper oxide nanoparticles with lysozyme. *J. Mater. Res. Technol.* **13**, 2066–2077 (2021).
95. Bigdeli, F. & Morsali, A. Synthesis ZnO nanoparticles from a new zinc (II) coordination polymer precursor. *Mater. Lett.* **64** (1), 4–5 (2010).
96. Poyraz, S. et al. One-step synthesis and characterization of polyaniline nanofiber/silver nanoparticle composite networks as antibacterial agents. *ACS Appl. Mater. Interfaces*. **6** (22), 20025–20034 (2014).
97. Belavi, P., Chavan, G., Naik, L., Somashekar, R. & Kotnala, R. Structural, electrical and magnetic properties of cadmium substituted nickel–copper ferrites. *Mater. Chem. Phys.* **132** (1), 138–144 (2012).
98. Pal, K., Elkodous, M. A. & Mohan, M. M. CdS nanowires encapsulated liquid crystal in-plane switching of LCD device. *J. Mater. Sci.: Mater. Electron.* **29** (12), 10301–10310 (2018).
99. Arora, N., Thangavelu, K. & Karanikolos, G. N. Bimetallic nanoparticles for Antimicrobial Applications. *Front. Chem.* **8**, 412 (2020).
100. Bakina, O. et al. Design and Preparation of silver–copper nanoalloys for Antibacterial Applications. *J. Cluster Sci.* **32** (3), 779–786 (2021).
101. Ashishie, P. B., Inah, B. E. & Ayi, A. A. Evaluation of antimicrobial activity of ionic liquid-assisted synthesis of monometallic silver and bimetallic copper-silver nanoparticles. *Int. J. Sci.* **7** (5), 25–31 (2018).
102. Eremenko, A. M., Petrik, I. S., Smirnova, N. P., Rudenko, A. V. & Marikvas, Y. S. Antibacterial and Antimycotic Activity of Cotton Fabrics, impregnated with Silver and Binary Silver/Copper Nanoparticles. *Nanoscale Res. Lett.* **11** (1), 28 (2016).
103. Paszkiewicz, M. et al. Synthesis and characterization of Monometallic (Ag, Cu) and bimetallic Ag-Cu particles for antibacterial and antifungal applications. *J. Nanomaterials*. **2016**, 2187940 (2016).
104. Ma, X., Zhou, S., Xu, X. & Du, Q. Copper-containing nanoparticles: mechanism of antimicrobial effect and application in dentistry-a narrative review. *Front. Surg.* **9**, 905892 (2022).
105. Gird, C. E., Costea, T. & Mitran, V. Evaluation of cytotoxic activity and anticancer potential of indigenous Rosemary (Rosmarinus officinalis L.) and oregano (Origanum vulgare L.) dry extracts on MG-63 bone osteosarcoma human cell line. *Romanian J. Morphology Embryol. = Revue Roumaine de Morphologie et embryologie*. **62** (2), 525–535 (2021).
106. Ioset, J. R., Brun, R., Wenzler, T., Kaiser, M. & Yardley, V. Drug screening for kinetoplastids diseases, A Training Manual for Screening in Neglected Diseases (2009).
107. Chunarkar-Patil, P. & Kaleem, M. Anticancer Drug Discovery Based on Natural Products: From Computational Approaches to Clinical Studies, 12(1) (2024).
108. Hu, T. et al. *Nanomedicines Overcoming Cancer Drug Resist.*, **14**(8) (2022).
109. Ali, O. M., Hasanin, M. S., Suleiman, W. B., Helal, E. E. H. & Hashem, A. H. Green biosynthesis of titanium dioxide quantum dots using watermelon peel waste: Antimicrobial, antioxidant, and anticancer activities. *Biomass Convers. Biorefinery*. **14** (5), 6987–6998 (2024).
110. Hashem, A. H. & El-Sayyad, G. S. Antimicrobial and anticancer activities of biosynthesized bimetallic silver-zinc oxide nanoparticles (Ag-ZnO NPs) using pomegranate peel extract. *Biomass Convers. Biorefinery* 1–13. (2023).

111. Yang, H., Zhang, X., Velu, P., Liu, X. & Vijayalakshmi, A. Enhanced green mediated synthesis of optimized Ag-Cu bimetallic nanoparticles using Leucas aspera and its application in anti-cancer activity against alveolar cancer. *Mater. Lett.* **313**, 131645 (2022).
112. Banik, M., Patra, M., Dutta, D., Mukherjee, R. & Basu, T. A simple robust method of synthesis of copper–silver core–shell nanoparticle: evaluation of its structural and chemical properties with anticancer potency. *Nanotechnology*. **29** (32), 325102 (2018).
113. Makada, H., Habib, S. & Singh, M. Bimetallic nanoparticles as suitable nanocarriers in cancer therapy. *Sci. Afr.* **20**, e01700 (2023).

Acknowledgements
The authors extend their appreciation to Researchers Supporting Project number (RSP2024R470), King Saud University, Riyadh, Saudi Arabia.

Author contributions
Amr H. Hashem, Mostafa A. Abdel-Maksoud, Saeedah M. Almutairi, Mohamed A. Ghorab, and Gharieb S. El-Sayyad suggested the research topic, investigated the article, planned the research methodology, wrote the original draft, and participated in data representation and article revising and editing. Sabiha Fatima, and Ahmed I. El-Batal participated in data representation and article revising and editing.

Funding
None.

Declarations

Compliance with ethical standards
Disclosure of potential conflict of interest: The authors declare that they have no conflict of interest.

Research involving Human Participation and/or Animals
Not applicable.

Informed consent
Not applicable.

Ethical approval
Not applicable.

Additional information
Correspondence and requests for materials should be addressed to A.H.H. or G.S.E.-S.

Reprints and permissions information is available at www.nature.com/reprints.

Publisher's note Springer Nature remains neutral with regard to jurisdictional claims in published maps and institutional affiliations.